

# Fusion-fission reactions with modified Woods-Saxon potential

Ning Wang,<sup>1,2,\*</sup> Kai Zhao,<sup>3</sup> Werner Scheid,<sup>1</sup> and Xizhen Wu<sup>3</sup>

<sup>1</sup>*Institut für Theoretische Physik der Universität, D-35392 Giessen, Germany*

<sup>2</sup>*College of Physics and Electronic Engineering,*

*Guangxi Normal University, Guilin 541004, P. R. China*

<sup>3</sup>*China Institute of Atomic Energy, Beijing 102413, P. R. China*

(Dated: November 5, 2018)

## Abstract

A modified Woods-Saxon potential model is proposed for a unified description of the entrance channel fusion barrier and the fission barrier of fusion-fission reactions based on the Skyrme energy-density functional approach. The fusion excitation functions of 120 reactions have been systematically studied. The fusion (capture) cross sections are well described with the calculated potential and an empirical barrier distribution. Incorporating a statistical model (HIVAP code) for describing the decay of the compound nucleus, the evaporation residue (and fission) cross sections of 51 fusion-fission reactions have been systematically investigated. Optimal values of some key parameters of the HIVAP code are obtained based on the experimental data of these reactions. The experimental data are reasonably well reproduced by the calculated results. The upper and lower confidence limits of the systematic errors of the calculated results are given.

---

\*Electronic address: wangning@gxnu.edu.cn

## I. INTRODUCTION

The production of superheavy nuclei as evaporation residues in fusion reactions is a field of very intense studies in the recent decades [1, 2, 3, 4, 5, 6]. So far, the superheavy elements  $Z = 110 \sim 116$  and 118 have been synthesized [7, 8, 9, 10, 11, 12, 13, 14, 15]. Theoretical support for these very time consuming experiments is vital in choosing the optimum target-projectile-energy combinations, and for the estimation of cross sections and identification of evaporation residues. A self-consistent microscopic dynamics model is still not yet available for practical studies of the whole fusion process from the capture to the decay of the heavy compound nuclei. Therefore, in the practical calculation of the evaporation residue cross section, the reaction process leading to the synthesis of superheavy nuclei is divided into two or three steps. Firstly, the projectile is captured by the target and a dinuclear system is formed which then evolves into the compound nucleus, and finally, the compound nucleus loses its excitation energy mainly by emission of particles and  $\gamma$ -ray and goes to its ground state. The simplified version of the evaporation residue cross section is given by

$$\sigma_{\text{ER}}(E_{\text{c.m.}}) = \sigma_{\text{cap}}(E_{\text{c.m.}})P_{\text{CN}}(E_{\text{c.m.}})W_{\text{sur}}(E_{\text{c.m.}}). \quad (1)$$

Here,  $\sigma_{\text{cap}}$ ,  $P_{\text{CN}}$  and  $W_{\text{sur}}$  are the capture cross section for the transition of the colliding nuclei over the entrance channel Coulomb barrier, the probability of the compound nucleus formation after the capture and the survival probability of the excited compound nucleus, respectively. There are several unsolved questions in each component of the right side of Eq.(1) which leave a certain margin of uncertainty in the estimates of the evaporation residue cross section [16]. In addition, there could be several parameters in the practical models which are hardly unambiguously determined by a very limited number of measured evaporation residue cross sections of superheavy nuclei. For example, the calculated formation probability  $P_{\text{CN}}$  of the compound nuclei for reaction  $^{58}\text{Fe}+^{208}\text{Pb}$  in [3] is about two orders of magnitude larger than that obtained in Ref.[4], both of the models can, however, reproduce the measured evaporation residue cross sections satisfactorily. Therefore, it is necessary to test and determine the interaction and parameters adopted in each component of Eq.(1) individually.

To study the three components in Eq.(1) individually, we first investigate the influence of the fission and quasi-fission on the fusion-fission reactions. It is generally thought that for systems with the compound-nuclear charge number  $Z_{\text{CN}}$  smaller than about 60, the fission

barrier is high enough to make fission an improbable decay mode at incident energies close to the fusion barrier [18]. Thus for these reactions,  $\sigma_{\text{ER}} \simeq \sigma_{\text{fus}} \simeq \sigma_{\text{cap}}$  holds at near-barrier energies. To see it more clearly, we present a schematic figure (Fig.1(a)). The horizontal and vertical axis denote the compound-nuclear charge number  $Z_{\text{CN}}$  and the mass asymmetry of the reaction system  $\eta = (A_2 - A_1)/(A_2 + A_1)$ , respectively. Here,  $A_1$  and  $A_2$  are the projectile and target masses. The fusion reactions in region I have  $P_{\text{CN}} \simeq W_{\text{sur}} \simeq 1$  as discussed before. There are quite a large number of experimental data of evaporation residue cross sections for the reactions in region I accumulated in recent decades, which makes it possible to establish a reliable model for systematic description of the capture process without the influence of fission and quasi-fission. For heavier compound systems the fission increases rapidly with the  $Z_{\text{CN}}^2/A_{\text{CN}}$  and the angular momentum. For sufficiently asymmetric systems with  $Z_{\text{CN}}$  well below 100 (systems in region II of Fig.1(a)), and at energies close to the fusion barrier, it is generally recognized that  $\sigma_{\text{fus}} = \sigma_{\text{ER}} + \sigma_{\text{FF}}$ . Here the  $\sigma_{\text{fus}}$ ,  $\sigma_{\text{ER}}$  and  $\sigma_{\text{FF}}$  are the cross sections for fusion, evaporation residue and fission, respectively. For systems in region II, it is thought that the quasi-fission barrier is high enough and thus  $P_{\text{CN}} \simeq 1$ . The available experimental data of the evaporation residue cross sections for reactions in region II are less than those in region I, but they seem to be much enough for a systematic investigation to test and determine some key parameters of a statistical model for calculating the survival probability  $W_{\text{sur}}$ , combining the model for describing the capture cross sections, without the influence of the quasi-fission. In addition, the measured fusion cross sections for reactions in region II can further test the theoretical model for calculating  $\sigma_{\text{cap}}$ . For  $Z_{\text{CN}}$  larger than about 100 (systems in region III of Fig.1(a)), quasi-fission occurs. Thus in the calculation of the evaporation residue cross sections for these reactions, the influence of quasi-fission should be taken into account ( $P_{\text{CN}} < 1$ ). In Fig.1(b) we illustrate this point more clearly. We show the contour plot of the quasi-fission barrier heights of the reactions with reaction partners along the  $\beta$ -stability line. Here, the height of the quasi-fission barrier is empirically estimated by the depth of the pocket of the entrance channel capture potential obtained with a modified Woods-Saxon potential which will be discussed in Sect.II. The height of the quasi-fission barrier decreases rapidly with the increase of the compound-nuclear charge, especially for symmetric target-projectile combination. For reactions with the same  $Z_{\text{CN}}$ , those with more asymmetric target-projectile combinations have higher quasi-fission barriers. It is expected that for sufficiently asymmetric systems the fusion probability  $P_{\text{CN}}$  is approximately equal

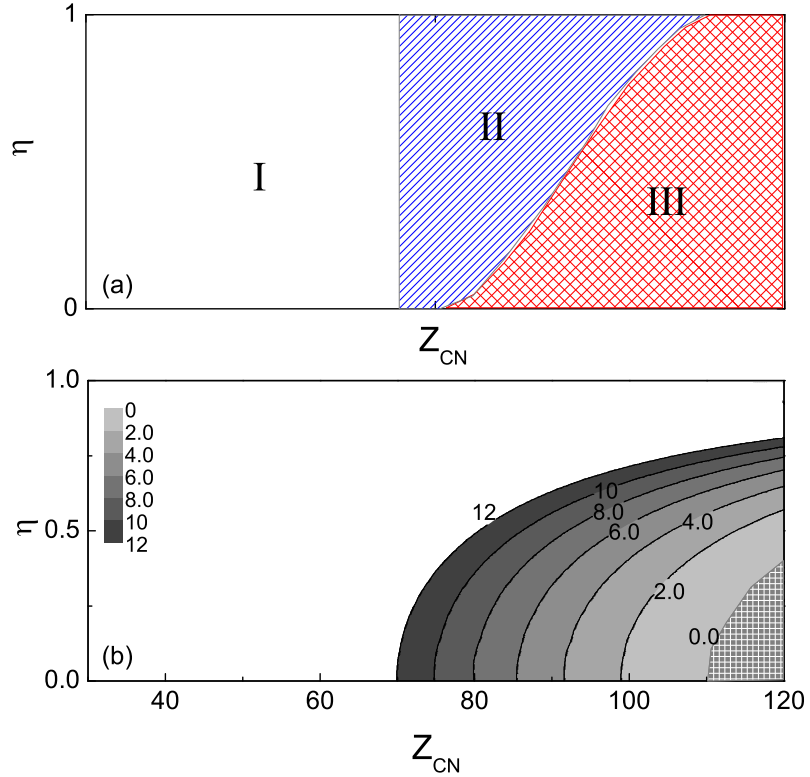


FIG. 1: (Color online) (a) A schematic figure for different types of fusion reactions. The horizontal and vertical axis denote the compound-nuclear charge number  $Z_{\text{CN}}$  and the mass asymmetry of the reaction system  $\eta = (A_2 - A_1)/(A_2 + A_1)$ , respectively. (b) Contour plot of the quasi-fission barrier heights obtained with a modified Woods-Saxon potential (which will be introduced in the next section) for reactions with nuclei along the  $\beta$ -stability line.

to one as mentioned above. If both  $\sigma_{\text{cap}}$  and  $W_{\text{sur}}$  can be predicted reliably, this would help to understand the dynamics of fusion and quasi-fission.

Based on above discussions, the emphasis of this paper is put on study of such fusion-quasi-fission reactions in which the quasi-fission is not important. To study this kind of reactions we employ a modified Woods-Saxon potential model based on the Skyrme energy density functional together with the extended Thomas-Fermi approach. This model was first proposed in [19] and a large number of fusion reactions have been described satisfactorily with the entrance channel potential. The potential between nuclei around the touching point can

be accurately evaluated with numerical algorithm [19]. Unfortunately, it is not so convenient for any practical application because one needs to evaluate numerically the microscopic densities of the interacting nuclei, the derivatives of these densities and the integrals. It is better to find an analytical expression for the potential. In this work we will present an analytical modified Woods-Saxon (MWS) form for the potential based on the numerical results. With the analytical MWS potential, both the fusion barrier and the fission barrier of a reaction system will be consistently studied. For calculation of  $W_{\text{sur}}$ , the well known standard statistical model (with HIVAP code [5, 18, 20]) is used. Then, the evaporation residue cross sections of a series of fusion-fission reactions will be investigated for a systematic test of the model and refining the parameters.

## II. MODIFIED WOODS-SAXON POTENTIAL AND SOME PARAMETERS OF HIVAP CODE

In this section, we first introduce an empirical nucleus-nucleus potential based on the Skyrme energy density functional within the extended Thomas-Fermi approach. Then, the statistical model HIVAP is briefly introduced and the influence of some key parameters is studied. Finally, a number of calculated results are compared with experimental data.

### A. Modified Woods-Saxon Potential and Fusion Cross Section

The nucleus-nucleus interaction potential reads as:

$$V(R) = V_N(R) + V_C(R). \quad (2)$$

Here,  $V_N$  and  $V_C$  are the nuclear and Coulomb interactions, respectively. We take  $V_C(R) = e^2 Z_1 Z_2 / R$ , and the nuclear interaction  $V_N$  to be of Woods-Saxon form with five parameters determined by fitting the entrance channel potentials obtained with the Skyrme energy density functional within the extended Thomas-Fermi (up to second order in  $\hbar$  [21]) approach proposed in [19]:

$$V_N(R) = \frac{V_0}{1 + \exp[(R - R_0)/a]}, \quad (3)$$

with [22]

$$V_0 = u_0 [1 + \kappa(I_1 + I_2)] \frac{A_1^{1/3} A_2^{1/3}}{A_1^{1/3} + A_2^{1/3}}, \quad (4)$$

TABLE I: Parameters of the potential.

	$r_0(fm)$	$c(fm)$	$u_0(MeV)$	$\kappa$	$a(fm)$
This work	1.27	-1.37	-44.16	-0.40	0.75
Ref.[22]			-46.07	-0.47	

and

$$R_0 = r_0(A_1^{1/3} + A_2^{1/3}) + c. \quad (5)$$

$I_1 = (N_1 - Z_1)/A_1$  and  $I_2 = (N_2 - Z_2)/A_2$  in Eq.(4) are the isospin asymmetries of projectile and target nuclei, respectively.

By varying the five free parameters  $u_0$ ,  $\kappa$ ,  $r_0$ ,  $c$  and  $a$  of the modified Woods-Saxon (MWS) potential, we minimize the relative deviation between the fusion barrier height obtained with the Skyrme energy-density functional with SkM\* [23] force and the barrier height of the MWS potential obtained with Eq.(2). The corresponding optimal values of these parameters are obtained at the minimum of the relative deviation. In this work, 66996 reactions with  $Z_1 Z_2 \leq 3000$  were used to determine the parameters of the modified Woods-Saxon potential. The obtained optimal values of the parameters are listed in Table I. Here we also list the potential depth parameters  $u_0$  and  $\kappa$  proposed in [22] for comparison. In [22] the nuclear interaction is taken as a Gaussian form and the potential parameters are also determined by the Skyrme interaction SkM\*. We find that the potential depth parameters obtained with the two approaches are close to each other.

With the modified Woods-Saxon potential together with the proposed empirical fusion barrier distribution in [19], the fusion cross sections and the mean barrier heights of a large number of reactions can be reproduced well [19, 24, 25, 26]. For the reader's convenience, the empirical barrier distribution is briefly introduced here. We assume the barrier distribution function  $D(B)$  to be a superposition of two Gaussian functions  $D_1(B)$  and  $D_2(B)$ ,

$$D_1(B) = \frac{\sqrt{\gamma}}{2\sqrt{\pi}b_1} \exp \left[ -\gamma \frac{(B - B_1)^2}{(2b_1)^2} \right] \quad (6)$$

and

$$D_2(B) = \frac{1}{2\sqrt{\pi}b_2} \exp \left[ -\frac{(B - B_2)^2}{(2b_2)^2} \right], \quad (7)$$

with

$$B_1 = B_c + b_1, \quad (8)$$

$$B_2 = B_c + b_2, \quad (9)$$

$$b_1 = \frac{1}{4}(B_0 - B_c), \quad (10)$$

$$b_2 = \frac{1}{2}(B_0 - B_c). \quad (11)$$

Here  $B_0$  is the barrier height from the modified Woods-Saxon potential. The effective barrier height is  $B_c = fB_0$  with the reduction factor  $f = 0.926$ . The quantity  $\gamma$  in  $D_1(B)$  is a factor which empirically takes into account the structure effects and has a value larger or equal to 0.5. For the fusion reactions with neutron-shell open nuclei but near the  $\beta$ -stability line and for the fusion reactions at energies near and above the barriers we set  $\gamma = 1$ . For the reactions with neutron-shell closed nuclei or neutron-rich nuclei an empirical formula for the  $\gamma$  values was proposed in [19]. For a more convenient discussion, we introduce the inverse of  $\gamma$  as an enhancement factor  $g = 1/\gamma$ . The larger the value of  $g$  is, the larger the fusion cross section at sub-barrier energies is. From the discussions in [19], we learn that for the reactions with neutron-shell closed nuclei we have  $0 < g < 1$  while for the reactions with neutron-rich nuclei  $1 < g \leq 2$ . With the proposed empirical barrier distribution, and the fusion radius  $R_{fus}$  and the curvature of the barrier  $\hbar\omega$  obtained with the modified Woods-Saxon potential, the fusion excitation function (or the capture excitation function of reactions in region III of Fig.1(a)) can be obtained (details in Refs. [19, 24])

$$\sigma_{fus}(E_{c.m.}) = \min[\sigma_1(E_{c.m.}), \sigma_{avr}(E_{c.m.})], \quad (12)$$

with

$$\sigma_1(E_{c.m.}) = \int_0^\infty D_1(B) \sigma_{fus}^{Wong}(E_{c.m.}, B) dB, \quad (13)$$

and

$$\sigma_{avr}(E_{c.m.}) = \int_0^\infty \left[ \frac{D_1(B) + D_2(B)}{2} \right] \sigma_{fus}^{Wong}(E_{c.m.}, B) dB. \quad (14)$$

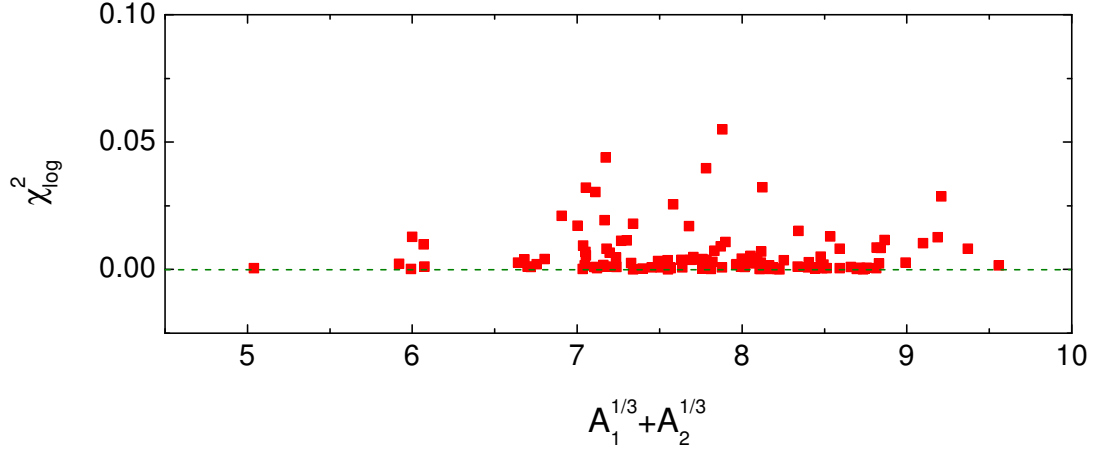


FIG. 2: (Color online) The average deviations  $\chi_{\log}^2$  for a total of 120 fusion reactions.  $A_1$  and  $A_2$  denote the projectile and target masses, respectively.

Where,  $\sigma_{fus}^{\text{Wong}}$  denotes Wong's formula [27] for penetrating an one-dimensional parabolic barrier,

$$\sigma_{fus}^{\text{Wong}}(E_{\text{c.m.}}, B_0) = \frac{\hbar\omega R_{fus}^2}{2E_{\text{c.m.}}} \ln \left( 1 + \exp \left[ \frac{2\pi}{\hbar\omega} (E_{\text{c.m.}} - B_0) \right] \right) \quad (15)$$

with the center-of-mass energy  $E_{\text{c.m.}}$ .  $B_0$ ,  $R_{fus}$  and  $\hbar\omega$  are the barrier height, radius and curvature, respectively. The influence of angular momentum in the entrance channel has already been taken into account in Wong's formula with the assumptions that the barrier position  $R_{fus}$  and the barrier curvature  $\hbar\omega$  do not change with angular momentum.

We have calculated the fusion (capture) excitation functions of 120 fusion reactions at energies near and above the barrier (with  $g = 1$ ) and their average deviations  $\chi_{\log}^2$  from the experimental data defined as

$$\chi_{\log}^2 = \frac{1}{m} \sum_{n=1}^m [\log(\sigma_{th}(E_n)) - \log(\sigma_{exp}(E_n))]^2. \quad (16)$$

Here  $m$  denotes the number of energy-points of experimental data, and  $\sigma_{th}(E_n)$  and  $\sigma_{exp}(E_n)$  are the calculated and experimental fusion (capture) cross sections at the center-of-mass energy  $E_n$  ( $E_n \geq B_0$ ), respectively. The calculated results for  $\chi_{\log}^2$  are shown in Fig.2. The average deviations of about 70% systems in  $\chi_{\log}^2$  are less than 0.005, with which we can estimate the systematic error of this approach for the description of the fusion (capture)



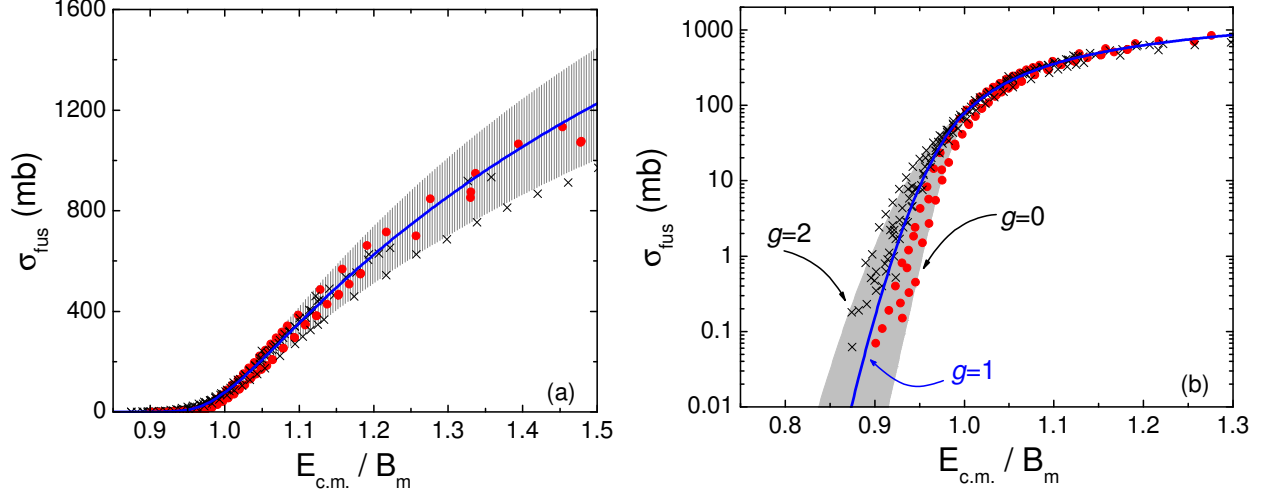


FIG. 3: (Color online) The fusion excitation functions of a series of reactions with  $^{16}\text{O}$  bombarding on medium mass targets. The incident energies are normalized by the mean barrier heights  $B_m$ . The fusion cross sections of these reactions are shown with linear and logarithmic scale in (a) and (b), respectively. The solid circles and crosses denote the experimental data of reactions with neutron-shell closed nuclei and with neutron-shell open nuclei, respectively. The solid curve denotes the calculation result with  $g = 1$ . The error bars in (a) are estimated with 18% of the fusion cross sections. The upper and lower limits of the cross sections in (b) are obtained with  $g = 2$  and  $g \simeq 0$ , respectively.

cross sections at energies near and above the barriers. A series of fusion reactions with  $^{16}\text{O}$  bombarding on medium mass targets such as  $^{144-154}\text{Sm}$  are studied with this approach, and the fusion excitation functions of these reactions are shown in Fig.3. The energy scale has been normalized by the mean barrier height  $B_m$  calculated with the proposed method by setting  $g = 1$  [26]. The scattered symbols denote the experimental data. The solid curve denote the calculated results with  $g = 1$ . The error bars in Fig.3(a) are estimated by 18%. In Fig.3(b), we notice that nearly all of the experimental data of sub-barrier energies are scattered in the region  $0 < g \leq 2$  as we defined in the proposed approach. The fusion cross sections (solid circles) of the reactions with neutron-shell closed nuclei at sub-barrier energies are systematically lower than the calculated results with  $g = 1$  which is consistent with our discussion mentioned previously. With  $g \simeq 0$  and  $g = 2$  we estimate the lower and upper limits of the fusion (capture) cross sections at sub-barrier energies respectively.

## B. Fission Barrier and Level Density Parameter in Evaporation Calculations

The calculations of the survival probabilities  $W_{\text{sur}}$  of the compound nuclei were performed with the statistical evaporation code called HIVAP which uses standard evaporation theory and takes into account the competition of  $\gamma$ -ray, neutron, proton,  $\alpha$ -particle emission with fission using angular-momentum and shape-dependent two-Fermi-gas-model level density formula[5]. Although it is a standard statistical model for describing the de-excitation process, one has to reconsider some parameters adopted for describing a wide range of fusion-fission reactions. The sensitive parameters involved are primarily fission barriers and level density parameters.

In the standard HIVAP code, the fission barrier at zero angular momentum is calculated by

$$B_f = B_f^{\text{Mac}} - S. \quad (17)$$

The macroscopic barrier  $B_f^{\text{Mac}}$  is usually described with a liquid-drop model refined by Cohen and Swiatecki [28], Sierk [29], and Dahlinger *et al.* [30]. The shell correction  $S$  is calculated from the difference of the experimental mass and the liquid-drop mass,  $S = M_{\text{exp}} - M_{\text{LD}}$ . In this code, the liquid-drop mass is calculated with the parameter set proposed by Myers and Swiatecki in 1967 [31], and the  $M_{\text{exp}}$  is in fact taken from the mass table of Möller-Nix [32] which was obtained with the finite range droplet model and has an rms deviation of only 0.656 MeV for 2149 measured masses of nuclei [33]. In the present work, we calculate the macroscopic fission barriers with the proposed modified Woods-Saxon (MWS) potential model in which the parameters of MWS potential are obtained based on the Skyrme energy density functional. The value of  $B_f^{\text{Mac}}$  is empirically estimated by the depth of the potential pocket, as shown as an example in Fig.4. This figure is for the  ${}_{102}^{256}\text{No}$  (formed in reaction  ${}_{48}\text{Ca}+{}_{208}\text{Pb}$ ) fissioning into two  ${}_{51}^{128}\text{Sb}$ . The obtained barrier is 1.74 MeV. The corresponding data from refs.[28, 29, 30] are 1.44, 1.02 and 1.19 MeV, respectively. The barrier for  ${}^{244}\text{Pu}$  from our method and from refs.[28, 29, 30] are 4.16, 5.17, 3.95 and 4.13 MeV, respectively. The deviations between our calculated results and the results of liquid-drop models for heavy nuclei are in a permitting region. For medium mass nuclei, our results are in agreement with those of refs.[34, 35] in which the reduction of the liquid-drop barriers was discussed.

We know that the nuclear shapes during fission are more elongated than during fusion. In this empirical approach, the neck and elongation of the system at fission configuration can not be described well in the sudden approximation. We concentrate on the height of the

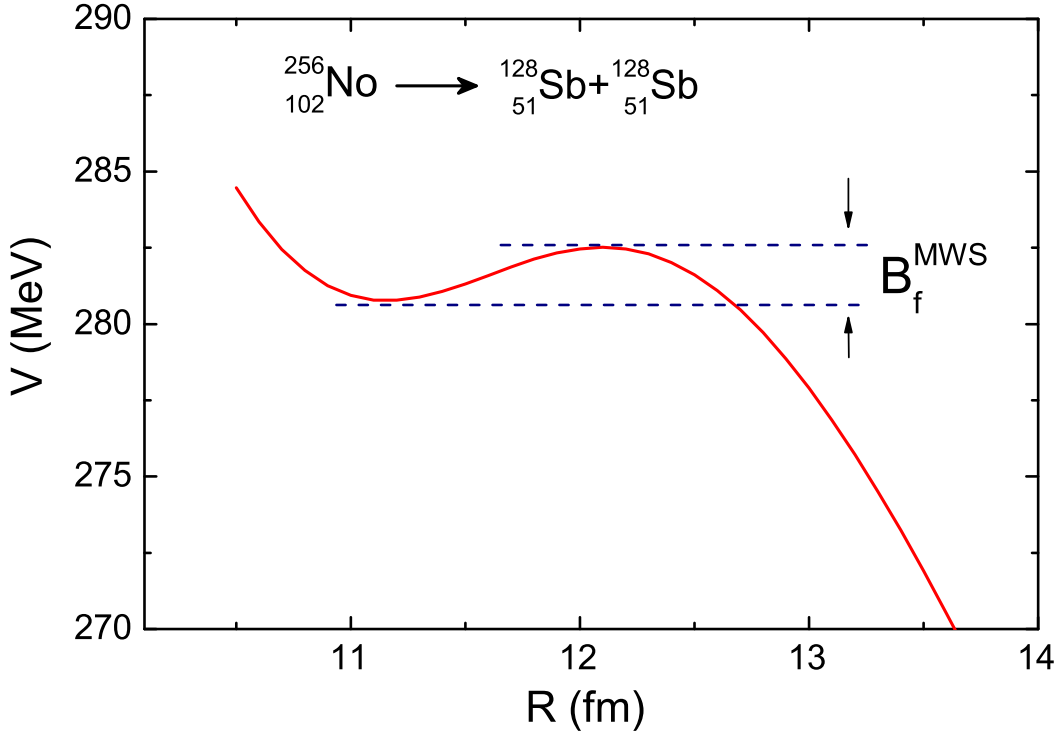


FIG. 4: (Color online) The macroscopic fission barrier  $B_f^{\text{MWS}}$  for  $^{256}_{102}\text{No}$  fissioning into two  $^{128}_{51}\text{Sb}$  obtained with the modified Woods-Saxon potential.

fission barrier in this method. We will systematically investigate 51 fusion-fission reactions with the fission barriers obtained with four different models (MWS potential model, Cohen-Swiatecki's[28], Sierk's[29] and Dahlinger's[30] methods). The results will be discussed in the following paragraph.

In this code, the level density is [20]

$$\rho(J, E^*) = \frac{1}{24} \left( \frac{\hbar^2}{2\theta} \right)^{3/2} (2J + 1) a^{1/2} U_J^{-2} \exp[2(aU_J)^{1/2}], \quad (18)$$

$$U_J = E^* - E_r(J). \quad (19)$$

Here  $E_r(J)$  is the yrast energy of either the equilibrium configuration (light-particle and  $\gamma$ -emission) or the saddle-point configuration (fission) and reads

$$E_r(J) = J(J + 1)\hbar^2/2I, \quad (20)$$

in which  $I$  is the moment of inertia. The level density parameter  $a$  is obtained from [18] as

$$a = \tilde{a}[1 + f(E^*)S/E^*], \quad (21)$$

with [36]

$$f(E^*) = 1 - \exp(-E^*/E_d) \quad (22)$$

with the shell damping energy  $E_d$  being 18.5MeV [20]. In the standard HIVAP code, the *smooth*, shell-independent level-density parameter reads

$$\tilde{a} = 0.04543 r_a^3 A + 0.1355 r_a^2 A^{2/3} B_S + 0.1426 r_a A^{1/3} B_K, \quad (23)$$

which takes into account the volume, surface and curvature dependence of the single-particle level density at the Fermi surface.  $B_S$  and  $B_K$  denote the surface and curvature factors defined in the droplet model [37]. For evaporation channels we set  $B_S = B_K = 1$ . For the fission channel, the values of  $B_S$  and  $B_K$  are tabulated as a function of the fissility parameter in [37]. The ratio  $\tilde{a}_f/\tilde{a}_n$  ( $\tilde{a}_f$  level density parameter for fission channel,  $\tilde{a}_n$  for neutron channel) is larger than 1. It decreases towards to an unit with the increase of the fissility parameter. The results of  $\tilde{a}_f/\tilde{a}_n$  for a series of nuclei in [20] can be well reproduced.  $r_a$  is the radius parameter found to be  $r_a = 1.153$  fm [20].

With this parametrization 51 fusion-fission reactions have been systematically investigated with the MWS, Cohen-Swiatecki's, Sierk's and Dahlinger's fission barriers, respectively, incorporating the proposed approach for describing the fusion (capture) cross sections (see Eq.(12)). Calculations of the fission and particle emission widths with the traditional statistical theory were introduced in [34]. The average deviation  $\chi_{\log}^2$  (see Eq.(16)) of the evaporation (and fission) cross sections from the experimental data for these reactions are listed in Table II. We find that the average deviation obtained with the MWS potential is much smaller than those obtained with the other barriers. By varying the volume, surface and curvature coefficients in Eq.(23) and the damping energy  $E_d$ , and searching for the minimum of  $\chi_{\log}^2$  with the MWS fission barriers, we find that the values proposed by Reisdorf [20] (adopted in the present work) are very close to the corresponding optimal ones. In some references the shell damping energy was written as  $E_d = k_0 A^{1/3}$  or similar forms [6, 39, 40]. We find that the minimal deviation is not much improved by changing the value of the coefficient  $k_0$ . Therefore, in our calculations we consequently keep Reisdorf's coefficients, Eq.(23), that contains only one empirically adjustable parameter  $r_a$ .

TABLE II: Average deviation of the evaporation (and fission) cross sections from experimental data for 51 fusion-fission reactions with  $r_a = 1.153$  fm.

model	Cohen-Swiatecki	Sierk	Dahlinger	MWS
$\chi_{\log}^2$	0.2295	0.2177	0.2373	0.1339

TABLE III: The minimal average deviation  $\chi_{\log}^2$  and the corresponding optimal value of  $r_a$  adopting different models for calculating the fission barriers.

model	Cohen-Swiatecki	Sierk	Dahlinger	MWS
$\chi_{\log}^2$	0.1813	0.1428	0.1642	0.1086
$r_a$	1.106	1.091	1.095	1.120

To determine the optimal value of  $r_a$ , we first study the reasonable range of  $r_a$ . The level density parameter is usually dependent on the nuclear mass number from  $A/8$  to  $A/12$  [6, 38, 39]. Fig.5 shows the level density parameter  $\tilde{a}$  as a function of nuclear mass number  $A$  adopting different values for  $r_a$  (with  $B_S = B_K = 1$ ). We estimate the variation region of  $r_a$  which ranges from about 1.075 to 1.250 fm according to  $A/12 \sim A/8$ . Through a variation of  $r_a$  we can find the optimal values of  $r_a$  for a certain model to describe the fission barriers. The optimal value of  $r_a$  could be different for different fission barrier models. Through systematical investigation of the minimal average  $\chi_{\log}^2$  of the 51 fusion-fission reactions, we search for the optimal parameters set (including the parameters of fission barrier and the  $r_a$  in level density parameter). The minimal average  $\chi_{\log}^2$  of the 51 reactions and the corresponding optimal values of  $r_a$  for the four fission barrier models are listed in Table III. By taking the optimal values of  $r_a$ , the average deviations  $\chi_{\log}^2$  from the experimental data get obviously smaller for all of these models, especially for the models of Sierk and Dahlinger. The deviation obtained by the modified Woods-Saxon potential is still the smallest one.

According to the formulas for the fission barrier and the level density parameter, one learns that a reasonable calculation of the shell correction  $S$  is crucial since the shell correction plays a role both for the fission barrier and for the level density parameter, especially for heavy systems. Therefore, it is interesting to compare the results with the shell corrections obtained by different approaches for searching for the optimal parameters set of the HIVAP code. The previous calculations discussed are based on the shell corrections obtained with

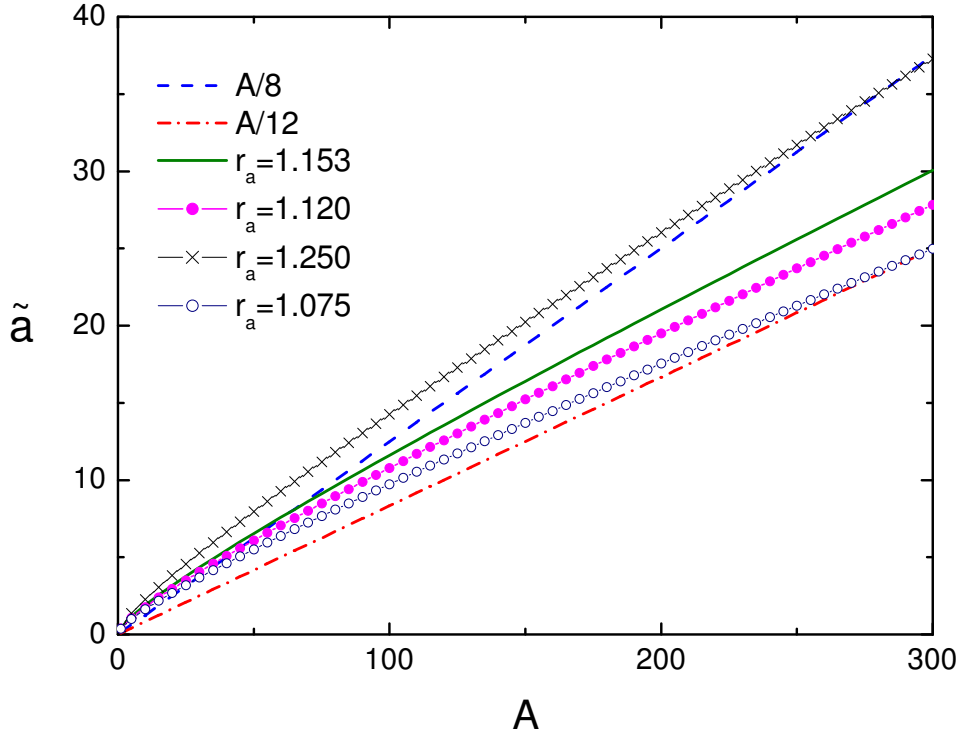


FIG. 5: (Color online) Level density parameter as a function of nuclear mass number  $A$ .

the 1967 parametrization of Mayers and Swiatecki [31] for  $M_{LD}$ . If we take the shell corrections of Möller-Nix based on the 1995 parametrization of the macroscopic (liquid-drop) energies of nuclei [32], the minimal deviation  $\chi_{\log}^2$  and the corresponding optimal  $r_a$  are 0.1877 and 1.252 fm with the Sierk's barrier, 0.1681 and 1.268 fm with the MWS fission barrier, respectively. Comparing with the results listed in Table III, one finds that using the shell corrections based on the 1967 parametrization of the liquid-drop energies  $M_{LD}$  of nuclei [31] the fusion-fission reactions studied in this work can be systematically better described with the present HIVAP code for  $W_{\text{sur}}$  incorporating the proposed approach for  $\sigma_{fus}$ . Finally, we obtain the optimal parameters set of the HIVAP code: MWS potential model for the fission barriers, with  $r_a = 1.120$  fm and together with the 1967 parametrization of the liquid-drop energies of nuclei for the shell corrections.

### C. Comparison between the Calculated Results and the Experimental Data

With the modified Woods-Saxon potential for the unified description of the entrance channel fusion barrier and the macroscopic fission barrier  $B_f^{\text{Mac}}$ , with  $r_a = 1.120$  fm, and together with the 1967 parametrization of Mayers and Swiatecki for the shell corrections, we obtained the deviations  $\chi_{\log}^2$  of the evaporation (and fission) cross sections from the experimental data for the 51 fusion-fission reactions which are shown in Fig.6. We find that 68.3% reactions have values smaller than 0.0714, with which we can estimate the upper and lower confidence limits of the systematic errors of the HIVAP code for  $W_{\text{sur}}$  (the values are  $1.85W_{\text{sur}}$  and  $W_{\text{sur}}/1.85$ , respectively). In the following figures, Fig.7 – Fig.12, we present the calculated results together with the systematic errors (the shades in the figures) of  $\sigma_{fus}$  and  $W_{\text{sur}}$ . The experimental data are also presented for comparison. From these figures, one finds that the experimental data can be systematically well reproduced (within about 2 times deviations) at energies near and above the fusion barriers.

Fig.13 shows calculated neutron evaporation residue cross sections for heavy systems with  $^{208}\text{Pb}$ . Because the quasi-fission has not been taken into account in these calculations yet, we find that the deviations from the experimental data increase exponentially with the increase of  $Z_{\text{CN}}$  (the positions of the peaks for the evaporation residues can be roughly reproduced). This implies that the quasi-fission plays an important role in the reactions leading to superheavy nuclei. With the proposed approach for  $\sigma_{\text{cap}}$  and  $W_{\text{sur}}$ , the ambiguity in predicting the probability of quasi-fission could be reduced.

### III. CONCLUSION AND DISCUSSION

In this work, we proposed a modified Woods-Saxon potential for a unified description of the entrance channel fusion barrier and the fission barrier of fusion-fission reactions which is based on the Skyrme energy-density functional approach. With the proposed potential for the fusion barriers, 120 heavy-ion fusion reactions have been systematically investigated together with the barrier penetration concept and an empirical barrier distribution. The experimental data for the fusion cross sections  $\sigma_{fus}$  can be well reproduced and the systematic errors are 18% at energies near and above the barriers. Incorporating a statistical model HIVAP for describing the decay of the compound nuclei, the evaporation residue (and fission) cross sections of 51 fusion-fission reactions have been systematically studied simultaneously to investigate and refine some key parameters of the HIVAP code such as the fission barrier and the level density parameter. With the optimal value of the radius pa-

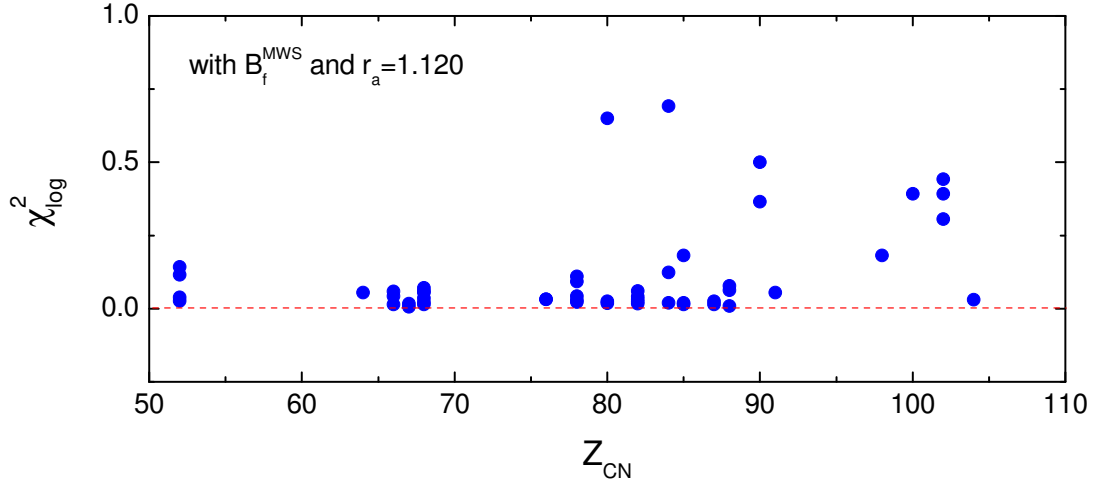


FIG. 6: (Color online) Deviations  $\chi_{\log}^2$  of the calculated evaporation (and fission) cross sections from the experimental data for 51 fusion-fission reactions.

parameter  $r_a = 1.120$  fm of the level density parameter, and with the fission barriers obtained by the proposed modified Woods-Saxon potential, the experimental data can be systematically reproduced reasonably well. The upper and lower confidence limits of the systematic errors of the calculated survival probabilities  $W_{\text{sur}}$  with the HIVAP code are  $1.85W_{\text{sur}}$  and  $W_{\text{sur}}/1.85$ , respectively. The influence of the shell corrections on the calculated results has been explored. The 1967 parametrization of Mayers and Swiatecki [31] for the macroscopic (liquid-drop) energies of nuclei gives better results in the case of these 51 reactions. For the systems leading to superheavy nuclei, the influence of quasi-fission increases rapidly with increasing the compound-nuclear charge number  $Z_{\text{CN}}$ . With the individual investigation of  $\sigma_{\text{cap}}$  and  $W_{\text{sur}}$ , the ambiguity of the prediction of the evaporation cross sections could be reduced, which is helpful in testing models for the formation probability  $P_{\text{CN}}$  of compound nuclei.

In the present work, the estimated systematic errors based on the enhancement factor  $0 < g \leq 2$  for the capture cross sections at sub-barrier energies are still large, especially for heavy systems. A precise prediction of the enhancement factor  $g$  and a reduction of the corresponding systematic errors are still required, especially for the "cold fusion" in which



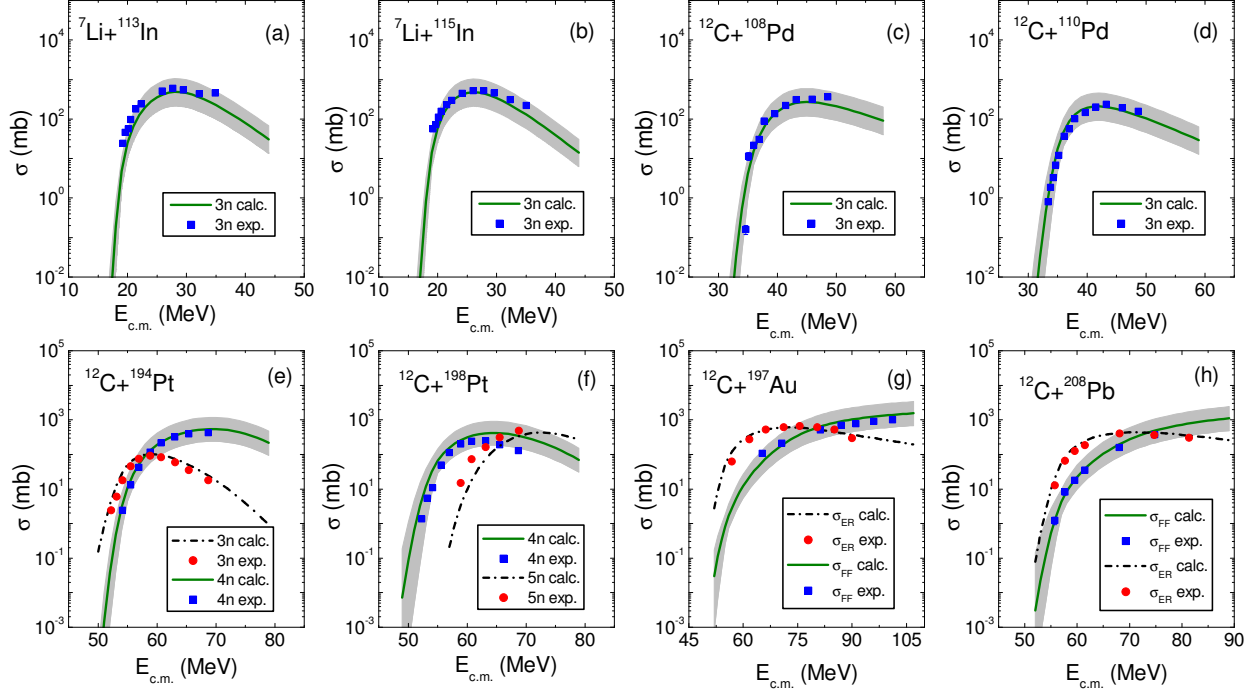


FIG. 7: (Color online) The cross sections of reactions  ${}^7\text{Li}+{}^{113,115}\text{In}$  [41],  ${}^{12}\text{C}+{}^{108,110}\text{Pd}$  [41],  ${}^{12}\text{C}+{}^{194,198}\text{Pt}$  [42],  ${}^{12}\text{C}+{}^{197}\text{Au}$  [43] and  ${}^{12}\text{C}+{}^{208}\text{Pb}$  [44].  $\sigma_{\text{FF}}$  denotes the fission cross section.  $\sigma_{\text{ER}}$  denotes the evaporation residue cross section (a sum over all evaporation channels). The shades in this and the following figures denote the systematic errors of the present approach (including both the systematic errors of  $\sigma_{\text{cap}}$  and those of  $W_{\text{sur}}$ ), if not otherwise stated.

the suitable incident energies for producing evaporation residues are near or lower than the average fusion barrier. For "hot fusion" systems, the suitable incident energies could be higher than the average fusion barrier, and thus the influence of  $g$  decreases since the capture cross sections are not very sensitive to the enhancement factor  $g$  at energies above the barrier. In addition, the influence of asymmetric fission and the time-dependent fission width [66] have not been taken into account yet. It is known that the nuclear dissipation influences the saddle-to-scission time and thus influences the competition between fission and particle evaporation. These effects are very important in fission dynamics but they are beyond the scope of this work. Work on these aspects is in progress.

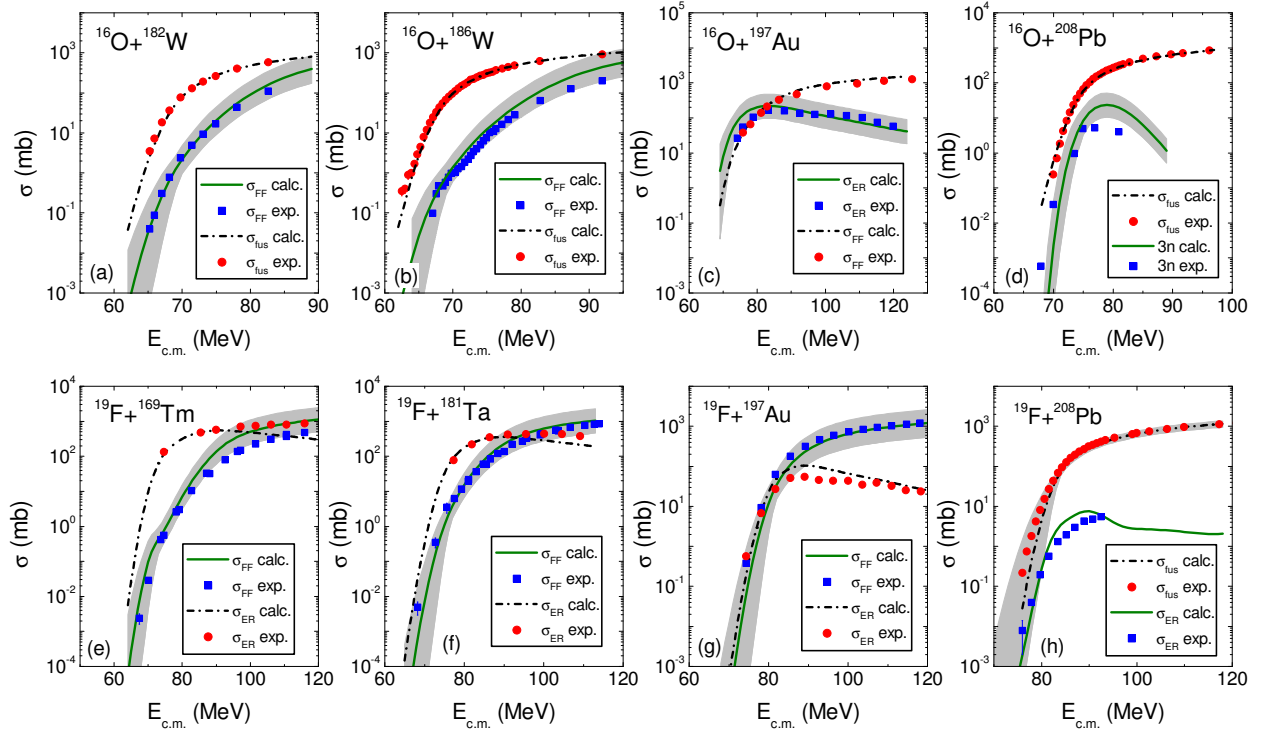


FIG. 8: (Color online) The cross sections of reactions  $^{16}\text{O}+^{182,186}\text{W}$  [45, 46],  $^{16}\text{O}+^{197}\text{Au}$  [43],  $^{16}\text{O}+^{208}\text{Pb}$  [47],  $^{19}\text{F}+^{169}\text{Tm}$  [48],  $^{19}\text{F}+^{181}\text{Ta}$  [48],  $^{19}\text{F}+^{197}\text{Au}$  [49] and  $^{19}\text{F}+^{208}\text{Pb}$  [50]. The shade in (h) denotes the systematic errors of the capture cross sections.

## ACKNOWLEDGEMENTS

One of the authors (N. Wang) thanks for the Alexander von Humboldt Foundation for support.

- 
- [1] Caiwan Shen, Grigori Kosenko, and Yasuhisa Abe, Phys. Rev. C **66**, 061602 (2002).
  - [2] Raj K. Gupta, Monika Manhas, et al., Phys. Rev. C **72**, 014607 (2005).
  - [3] V. I. Zagrebaev, Phys. Rev. C **64**, 034606 (2001).
  - [4] G. G. Adamian, et al., Nucl. Phys. A **633**, 409 (1998).
  - [5] W. Reisdorf and M. Schädel, Z. Phys. A **343**, 47 (1992).
  - [6] Z. Feng, G. Jin, F. Fu and J. Li, Nucl. Phys. A **771**, 50 (2006).
  - [7] S. Hofmann, V. Ninov, F.P. Hessberger et al., Z. Phys. A **350**, 277 (1995).
  - [8] S. Hofmann, V. Ninov, F.P. Hessberger et al., Z. Phys. A **350**, 281 (1995).

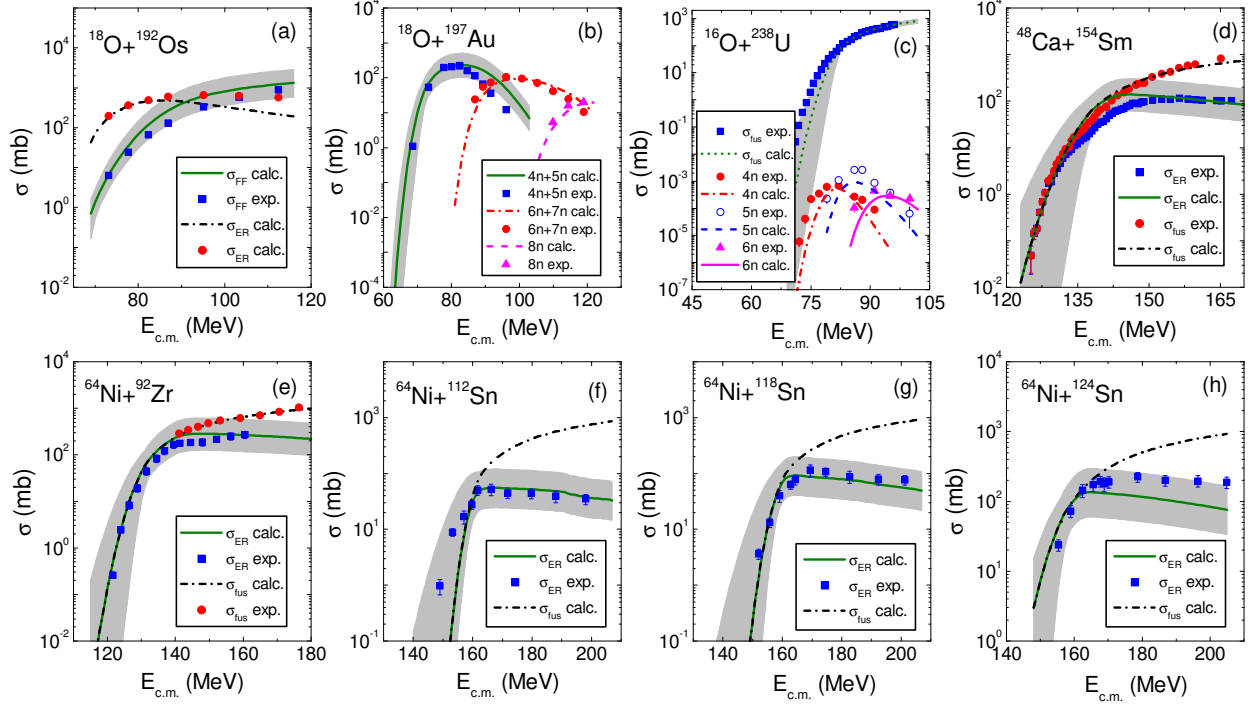


FIG. 9: (Color online) The cross sections of reactions  $^{18}\text{O}+^{192}\text{Os}$  [48],  $^{18}\text{O}+^{197}\text{Au}$  [51],  $^{48}\text{Ca}+^{154}\text{Sm}$  [52],  $^{16}\text{O}+^{238}\text{U}$  [53],  $^{64}\text{Ni}+^{92}\text{Zr}$  [54],  $^{64}\text{Ni}+^{112,118,124}\text{Sn}$  [55]. The shade in (c) denotes the systematic errors of the capture cross sections.

- [9] S. Hofmann and G. Mnzenberg, *Rev. Mod. Phys.* **72**, 733 (2000).
- [10] Yu. Ts. Oganessian, V. K. Utyonkov, et al., *Phys. Rev. C* **62**, 041604(R) (2000).
- [11] Yu. Ts. Oganessian, V. K. Utyonkov, et al., *Phys. Rev. C* **63**, 011301(R) (2000).
- [12] Yu. Ts. Oganessian, V. K. Utyonkov, et al., *Phys. Rev. C* **69**, 021601(R) (2004).
- [13] Yu. Ts. Oganessian, V. K. Utyonkov, et al., *Phys. Rev. C* **70**, 064609 (2004).
- [14] Kosuke Morita, Kouji Morimoto, et al., *J. Phys. Soci. Japan* **73**, 2593 (2004).
- [15] Yu. Ts. Oganessian, V. K. Utyonkov, et al., *Phys. Rev. C* **74**, 044602 (2006).
- [16] K. Siwek-Wilczynska, I. Skwira, et al., *Phys. Rev. C* **72**, 034605 (2005).
- [17] H. J. Krappe, J. R. Nix and A. J. Sierk, *Phys. Rev. C* **20**, 992 (1979).
- [18] W. Reisdorf, F. P. Hessberger, et al., *Nucl. Phys. A* **444**, 154 (1985).
- [19] Min Liu, Ning Wang, Zhuxia Li, Xizhen Wu and Enguang Zhao, *Nucl. Phys. A* **768**, 80 (2006).
- [20] W. Reisdorf, *Z. Phys. A* **300**, 227 (1981).
- [21] M. Brack, C. Guet, H.-B. Hakanson, *Phys. Rep.* **123**, 275 (1985).
- [22] A. Dobrowolski, K. Pomorski and J. Bartel, *Nucl. Phys. A* **729** 713 (2003).

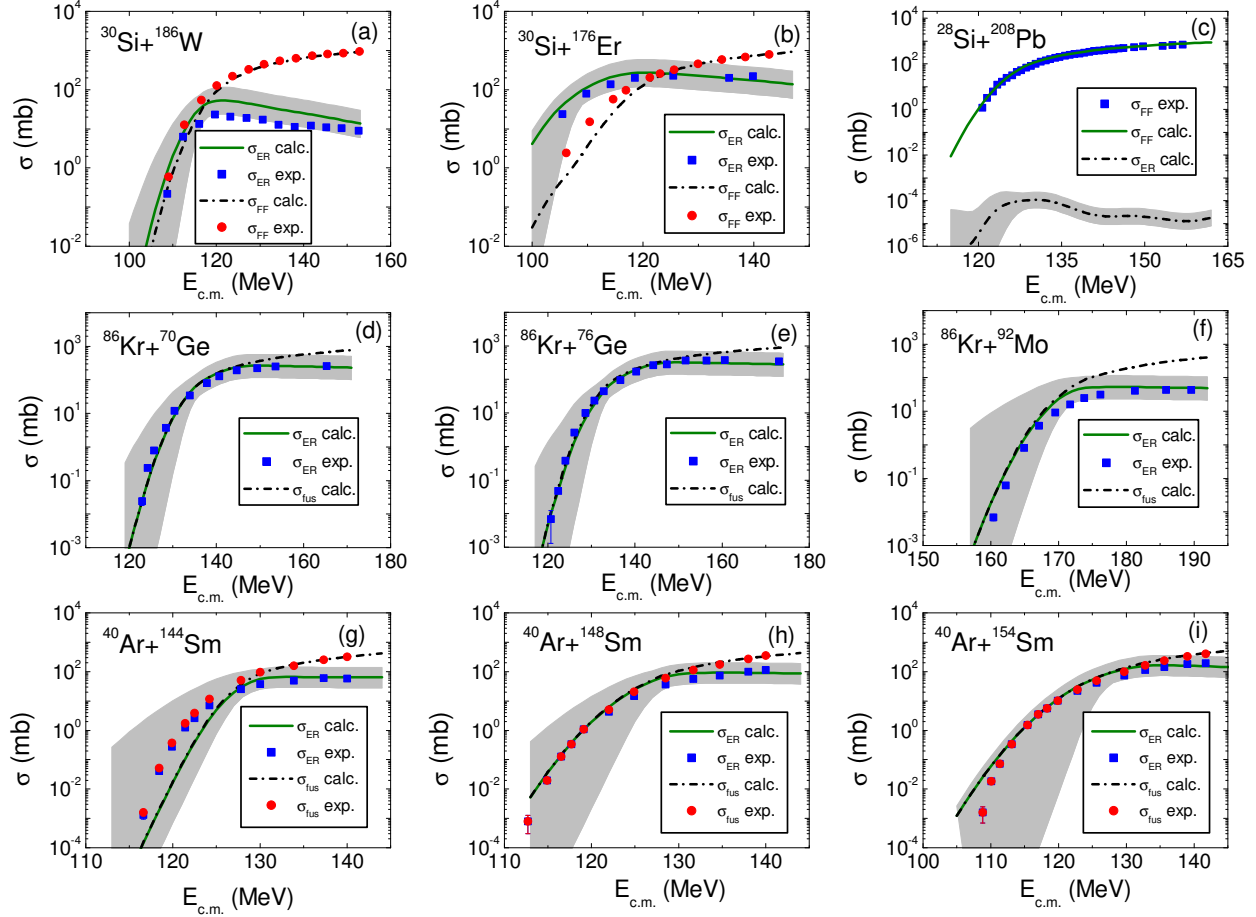


FIG. 10: (Color online) The cross sections of reactions  $^{30}\text{Si}+^{186}\text{W}$  [49],  $^{30}\text{Si}+^{176}\text{Er}$  [56],  $^{28}\text{Si}+^{208}\text{Pb}$  [57],  $^{86}\text{Kr}+^{70,76}\text{Ge}$  [18] and  $^{86}\text{Kr}+^{92}\text{Mo}$  [18],  $^{40}\text{Ar}+^{144,148,154}\text{Sm}$  [58].

- [23] J. Bartel, Ph. Quentin, M. Brack, C. Guet and H.B. Hakansson, Nucl. Phys. A **386**, 79 (1982).
- [24] Ning Wang, Xizhen Wu, Zhuxia Li, Min Liu, and Werner Scheid, Phys. Rev. C **74**, 044604 (2006).
- [25] Ning Wang, Zhuxia Li and Werner Scheid, J. Phys. G: Nucl. Part. Phys. **34** (2007) 1935.
- [26] TIAN Jun-Long, WANG Ning, LI Zhu-Xia, Chin. Phys. Lett. **24**, 905 (2007).
- [27] C.Y.Wong, Rev. Lett. **31**, 766 (1973).
- [28] S. Cohen, W.J. Swiatecki. Ann. Phys. (N.Y.) **22**, 406 (1963).
- [29] A. Sierk, Phys. Rev. C **33**, 2039 (1986).
- [30] M. Dahlinger, D. Vermeulen and K.-H. Schmidt, Nucl. Phys. A**376**, 94 (1982).
- [31] W. D. Myers and W. J. Swiatecki, Ark. Fys. **36**, 342 (1967).
- [32] P. Möller, J. R. Nix, W. D. Myers, W. J. Swiatecki At. Data and Nucl. Data Tables **59**, 185 (1995).

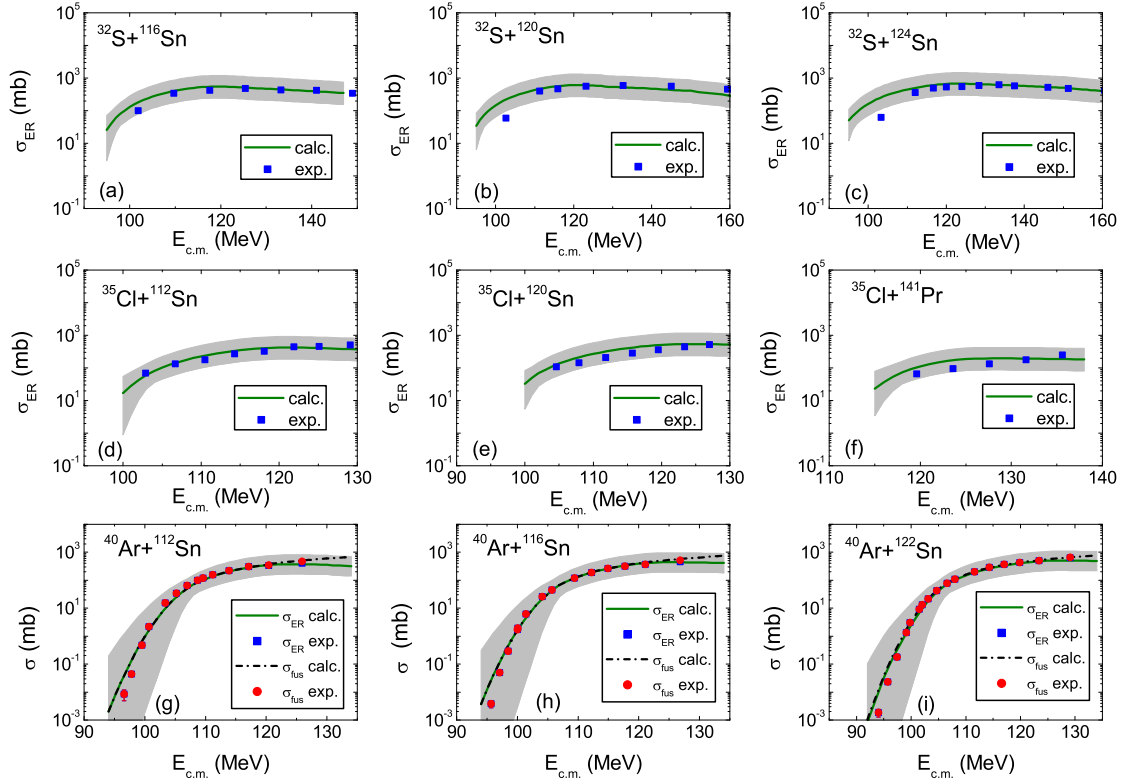


FIG. 11: (Color online) The evaporation residue cross sections of reactions  $^{32}\text{S}+^{116,120,124}\text{Sn}$  [59],  $^{35}\text{Cl}+^{112,120}\text{Sn}$  [60] and  $^{35}\text{Cl}+^{141}\text{Pr}$  [60],  $^{40}\text{Ar}+^{112,116,122}\text{Sn}$  [58].

- [33] F. Buchinger and J. M. Pearson, Phys. Rev. C **72**, 057305 (2005).
- [34] M.Beckerman and M.Blann, Phys. Rev. Lett. **38**, 272 (1977); Phys. Lett. B **68**, 31 (1977).
- [35] M.Beckerman and M.Blann, Phys. Rev. C **17**, 1615 (1978).
- [36] A. V. Ignatyuk, G. N. Smirenkin and A. S. Tishin, Yad. Fiz. 21, 485 (1975) [Sov. J. Nucl. Phys. **21**, 255 (1975)].
- [37] W. D. Myers and W. J. Swiatecki, Ann. Phys. **84**, 186 (1974).
- [38] J. L. Wile, D. L. Coffing, et al., Phys. Rev. C **51**, 1693 (1995).
- [39] G. G. Adamian, N. V. Antonenko, and W. Scheid, Phys. Rev. C**69**, 011601(R) (2004).
- [40] S. F. Mughabghab and C. Dunford, Phys. Rev. Lett. **81**, 4083 (1998).
- [41] O. A. Capurro, D. E. DiGregorio, et al., Phys. Rev. C **53**, 1301 (1996).
- [42] A. Shrivastava, S. Kailas, et al., Phys. Rev. C **63**, 054602 (2001).

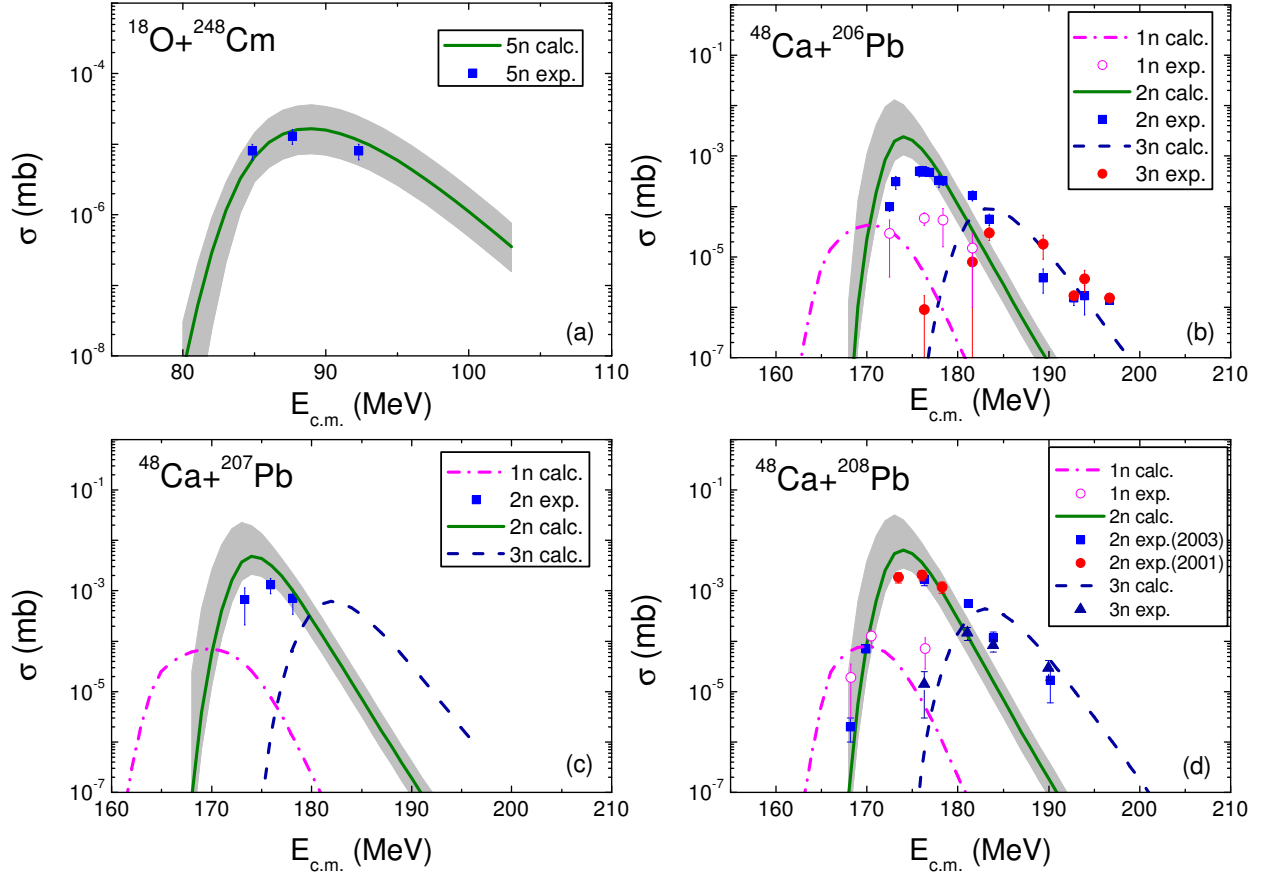


FIG. 12: (Color online) The cross sections of reactions  $^{18}\text{O}+^{248}\text{Cm}$  [61],  $^{48}\text{Ca}+^{206,207,208}\text{Pb}$  [62, 63]. The quasi-fission is not taken into account in the calculation.

- [43] S. Baba, K. Hata, et al., *Z. Phys. A* **331**, 53 (1988).
- [44] S. Santra, P. Singh, et al., *Phys. Rev. C* **64**, 024602 (2001).
- [45] D. J. Hinde, W. Pan, et al., *Phys. Rev. C* **62**, 024615 (2000).
- [46] J. R. Leigh, M. Dasgupta, et al., *Phys. Rev. C* **52**, 3151 (1995).
- [47] V. I. Zagrebaev, et al., *Phys. Rev. C* **65**, 014607 (2001); C. R. Morton, et al., *Phys. Rev. C* **60**, 044608 (1999).
- [48] R.J. Charity, J. R. Leigh, et al., *Nucl. Phys. A* **457**, 441 (1986).
- [49] D. J. Hinde, A. C. Berriman, et al., *J. Nucl. Radiochem. Sci.*, **3**, 31 (2002).
- [50] D. J. Hinde, A. C. Berriman, et al., *Phys. Rev. C* **60**, 054602 (1999).
- [51] L. Corradi, B. R. Behera, et al., *Phys. Rev. C* **71**, 014609 (2005).
- [52] M. Trotta, A. M. Stefanini, et al., *Eur. Phys. J. A* **25**, 615 (2005).
- [53] K. Nishio, H. Ikezoe, et al., *Phys. Rev. Lett.* **93**, 162701 (2004).

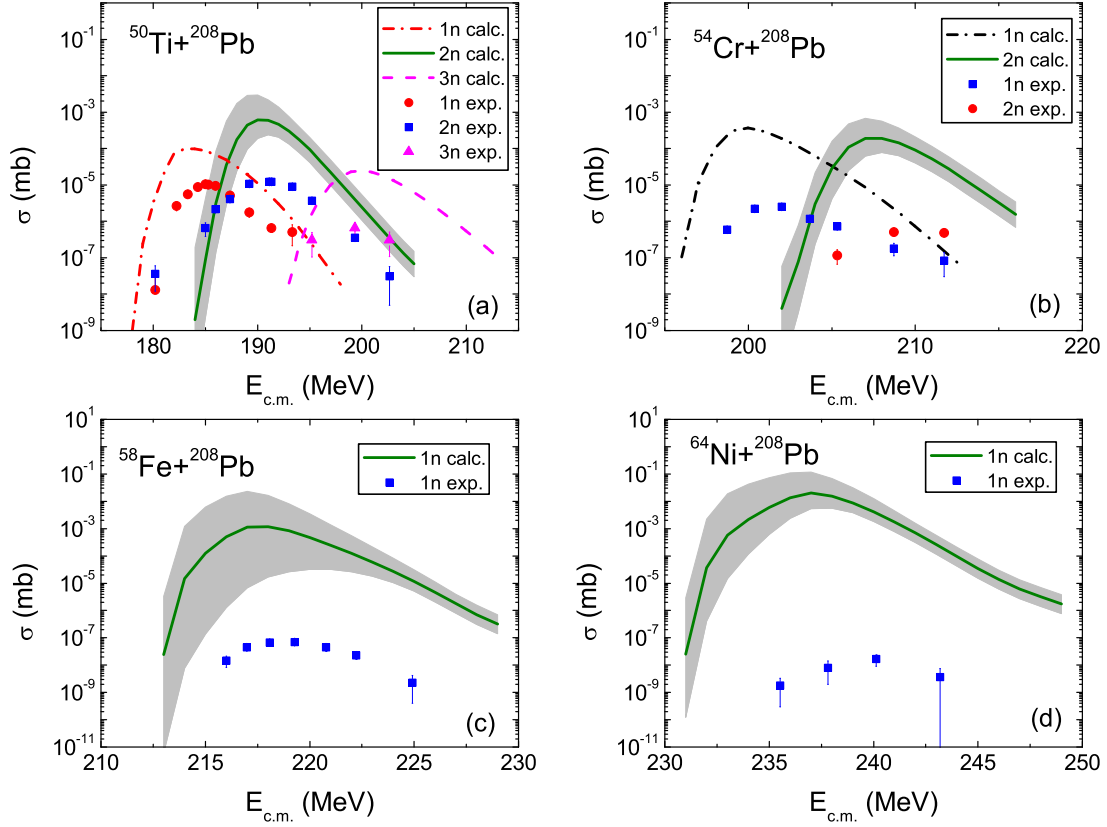


FIG. 13: (Color online) The neutron evaporation residue cross sections of heavy reactions with  $^{208}\text{Pb}$  target [64, 65]. The quasi-fission is not taken into account in the calculation.

- [54] A. M. Stefanini, et al., Nucl. Phys. A **548**, 453 (1992); F. L. H. Wolfs, et al, Phys. Rev. C **39**, 865 (1989).
- [55] J. F. Liang, D. Shapira, et al., Phys. Rev. C **75**, 054607 (2007).
- [56] D. J. Hinde et al., Nucl. Phys. A **398**, 308 (1983).
- [57] D. J. Hinde, C. R. Morton, et al., Nucl. Phys. A **592**, 271 (1995).
- [58] W. Reisdorf et al., Nucl. Phys. A **438**, 212 (1985).
- [59] H. Ernst, W. Henning, et al., Phys. Rev. C **29**, 464 (1984).
- [60] P. David, J. Bisplinghoff, et al., Nucl. Phys. A **287**, 179 (1977).
- [61] Y. Nagame, M. Asai, et al., J. Nucl. Radiochem. Sci. **3**, 85 (2002).
- [62] Yu. Ts. Oganessian, V. K. Utyonkov, et al., Phys. Rev. C **64**, 054606 (2001).

- [63] E.V.Prokhorova, E.A.Cherepanov, M.G.Itkis, et al, arXiv:nucl-ex/0309021.
- [64] S. Hofmann et al., Nucl. Phys. A **734**, 93 (2004).
- [65] K. Morita, K. Morimoto, D. Kaji et al., Nucl. Phys. A **734**, 101 (2004).
- [66] B. Jurado, C. Schmitt, K.-H. Schmidt, et al., Nucl. Phys. A **747**, 14 (2005).